Annexure – XI

Final Report Assessment / Evaluation Certificate

(Two Members Expert Committee Not Belonging to the Institute of Principal Investigator)

(to be submitted with the final report)

It is certified that the final report of Major Research Project MRP-MAJOR-BIOT-2013-38513 entitled" Potential anti-cancer...cell lines " by Dr./Prof. MAHUYA SENGUPTA Dept. of BIOTECHNOLOGY has been assessed by the committee consisting the following members for final submission of the report to the UGC, New Delhi under the scheme of Major Research Project.

Comments/Suggestions of the Expert Committee:-

After carefully evaluating the final report of the project entitled 'Potential anti-cancer property of arsenic nano-particles: a study of its anti-cancer efficacy and underlying mechanism using cancer cell lines' as submitted to UGC & the 3 publication generated thereof, Said documents were found Satisfactory.

Name & Signatures of Experts with Date:-

Name of Expert	University/College name	Signature with Date
1. Dr. Dolly Roy	Silchar Medical College + Hospital	Dolly Roy 29/7/24
2. Dr. S.L. Kothari	NIT Silchar	29/7/24

It is certified that the final report has been uploaded on UGC-MRP portal on 2019.

It is also certified that final report, Executive summary of the report, Research documents, monograph academic papers provided under Major Research Project have been posted on the website of the University/College.

(Registrar/Principal)

Seal

Registrar
Assam University, Silchar

c/167

Progress report and results achieved from July 2015 to June 2018:

Title: Potential anti-cancer property of arsenic nanoparticles: a study of its anti-cancer efficacy and the underlying mechanism using cancer cell lines

Mahuya Sengupta 26/6/2018

Executive summary:

Cancer is a major cause of devastating health outcomes and economic constraints in human life. Globally, cancer rates are increasing at a distressing rate. While intensive efforts have been made for the treatment of cancer, this disease is still the second leading cause of death in many countries. While intensive efforts have been made for the treatment of cancer, the recent therapies have some severe side effects such as permanent hair loss, fetal damage, skin problems, and secondary malignancies – the radiation itself is the source of mutations in healthy genes and can cause cancer.

Arsenic trioxide (ATO, As_2O_3) is used under the brand name 'ARSENOX, and 'TRISENOX®, as a chemotherapeutic drug for acute promyelocytic leukemia. However, expanding its use to the solid tumor is restricted because of its rapid renal clearance and requirement of the high dose which is associated with serious side effects affecting healthy organs as well. Our study aimed to address these limitations of ATO by synthesizing biocompatible albumin coated arsenic trioxide nanoparticles (msa-ATONPs) in order to increase their therapeutic efficiency and also target solid tumors in a murine model of fibrosarcoma. The designed nanostructure could target the solid tumors by albumin-mediated accumulation, where lysosomal catabolism of albumin exposes the nanoparticle cargo into the tumor microenvironment.

Experimentally, we compared the antiproliferative and oxidative mechanism of MSA-ATONPs with ATO in the cancer cell line MCF7. Also, i*n vivo* experiments were conducted to determine a sub-toxic dose capable of subsequent accumulation in the solid tumors in mice.

Findings from *in vitro* experiments showed an increased chemotherapeutic efficacy of the albumin-coated nanoparticle in MCF7 while *in vivo*, the transmission electron micrographs of the tumor tissue showed albumin-mediated endocytosis of the MSA-ATONPs. TEM micrographs also demonstrate membrane invaginations, blebbing and formation of pyknotic nuclei, confirming the proapoptotic nature of the nanoparticles.

Mahuya Sengupta 26/9/2018

Signature of the Principal Investigator

(Seal)

Assistant Professor
Department of Biotechnology
Assam University
Silchar-788011

16.11.18

Signature of the Registrar

(Seal)

कुलसचिव
Registrar
असम विश्वविद्यालय सिलचर
Assam University Silchar

INTRODUCTION

Cancer remains one of the most dangerous diseases affecting a large number of people worldwide every year. Even after profound cancer therapy, cases of cancer relapse and drug resistance are important, however, the immune response to such therapies is often reliant on the immunogenicity of a tumor[1]. Tumors are immunogenic, meaning; they elicit immune responses mostly mediated by both lymphocytes and monocytes. Further analysis revealed that the immunogenicity of the tumor depends on its antigenicity, recognized by the T- cells and several other immunomodulatory factors that are produced either by tumor cells or host cells in the tumor microenvironment[2]. Many immunomodulatory mechanisms operate in tumors. Most of them inhibit anti-tumor immunity. Epidemiological studies have provided definitive evidence that growing tumors in cancer patients can elicit a protective immune response which can slow down but not reverse the tumor growth[3].

As cancer cell can camouflage and present as self to the host immune system, a switch among macrophage takes place which hypnotizes them to act for the tumor cells contributing to their proliferation. However there has been reports of re-educating these macrophages and bringing back their senses to work for the immune system in controlling the malignancies of cancer or tumorigenic cells [2].Recent and valid evidence suggests that macrophages are monocytes cells plays a great role in controlling the malignancies of cancer or tumorigenic cells [2]. In this regard, chemo-immunotherapy is found to have a promising therapeutic strategy in dealing with various types and stages of cancer, designed in such a way, to gain effective and high cure rate.

HYPOTHESIS

The present study proposes to use a low-toxicity nano-formulation of arsenic in studying its anti-cancer efficacy and the underlying mechanism using cancer cell lines and murine fibrosarcoma.

The novel nanoparticle formulation of As(0) As_2(III)O3, in which the Arsenic is stabilized as a nanoparticulate precipitate and coated with serum albumin. The resultant arsenic "nano particles" are stable under physiologic conditions but undergo triggered drug release when the pH is lowered to endosomal/lysosomal levels. Cellular uptake and antitumor efficacy of these arsenic nanoparticles will be assayed in Jurkat T cells, HeLa cells, as well as ER-negative human breast (MCF-7) tumor cells and also in murine fibrosarcoma and lymphoma model through ELISA, western blotting, immunofluorescence, and cytotoxicity studies.

OBJECTIVES

1. Synthesis of As2O3 nanoparticles and their characterization and generation of efficient target-specificity.

2. Determination of cell viability and cytotoxicity after NP administration on various cancer cell lines exposed to NP along with colony forming assays.

3. Studies on apoptosis and DNA damage.

4. Studies on cytotoxicity and ROS generation after NP treatment in drug resistant cancer cells.

5.A profile of the proinflammatory cytokines that would give an insight into the molecular mechanism involved

RESULTS

Mahuya Sengupta 26/9/2018
Assistant Professor
Department of Biotechnology
Assam University
Silchar-1

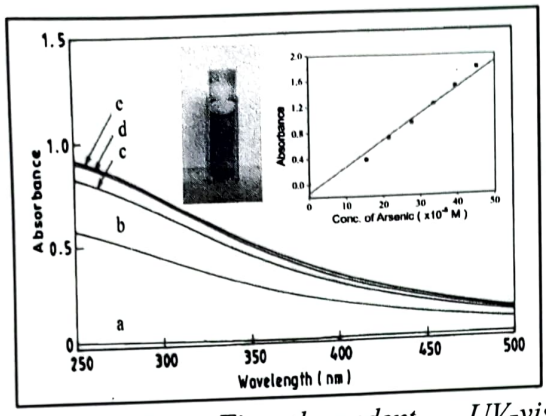

Figure 1: Time-dependent UV-vis absorption spectroscopic study on As(0) formation (Conc. 23.8 □ 10-5 M): (curve a) 0 min, (curve b) 30 min, (curve c) 60 min, (curve d) 0 min, and (curve e) 120 min. Inset: Calibration of As(0) at 300 nm.

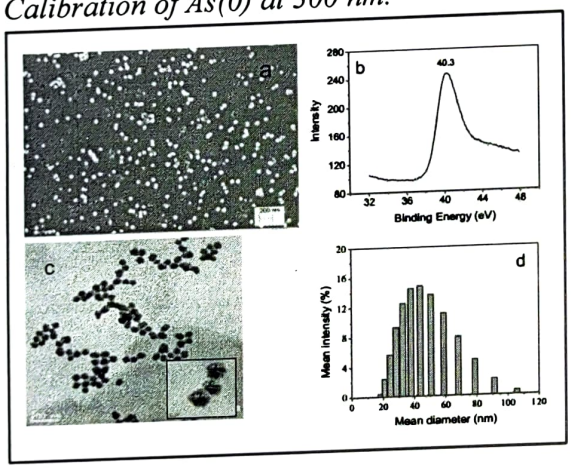

Figure 2: Characterization of As(0) nanoparticles: (a) SEM image; (b) XPS spectrum showing As 3d band; (c) TEM image (Inset: High resolution TEM image of selected nanoparticles); (d) DLS analysis

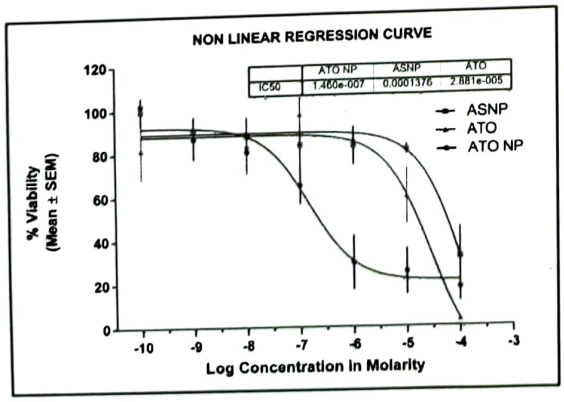

Figure 3: AsNP induces cytotoxicity on RAW 264.7 cell in a dose dependent manner. IC50 values were found at concentrations of 1.4x10-7 M for ATONP, 1.3x10-4 M for AsNP 2.8x10-5 M. Based on IC50 value, three doses were selected (0.5μM, 1μM and 5μM) respectively.

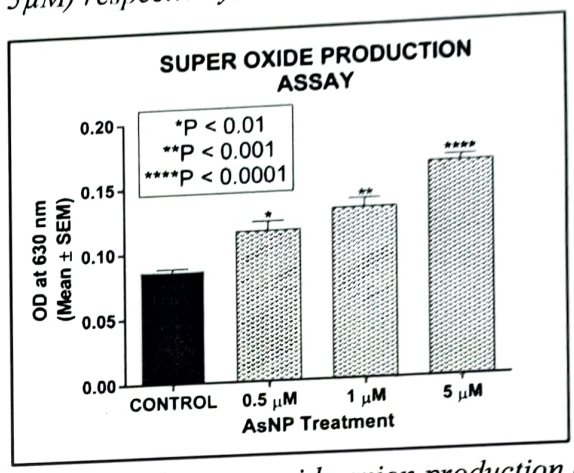

Figure 4: The superoxide anion production on RAW 264.7 cell showing a dose dependent increase from 0.086±0.002082 OD to 0.1633 ± 0.004410 OD for the group treated with highest dose of AsNP.

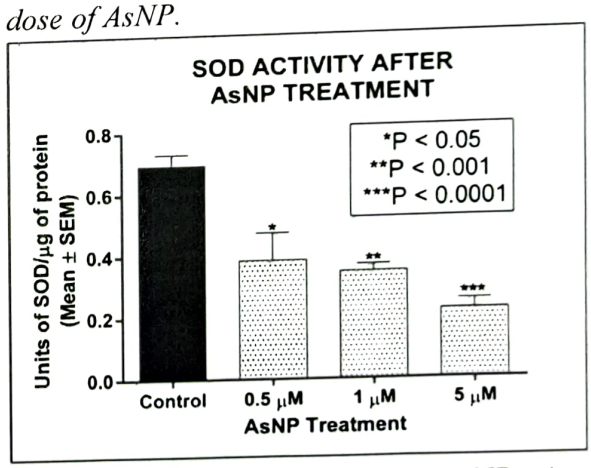

Figure 5: Treatment with AsNP in stimulated RAW 264.7 macrophage cell down regulated the antioxidant activity of the enzyme SOD

Mahuya Sengupta 26/9/2018

Assistant Professor
Department of Biotechnology
Assam University
Silchar-788011

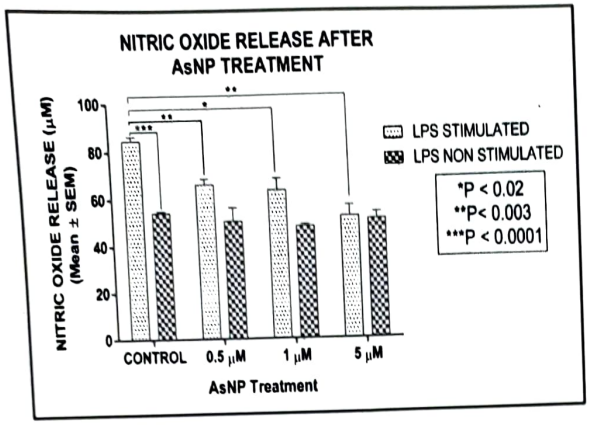

Figure 6: Treatment with AsNP prevented the production and release of Nitric Oxide after stimulating RAW 264.7 macrophage cell with LPS.

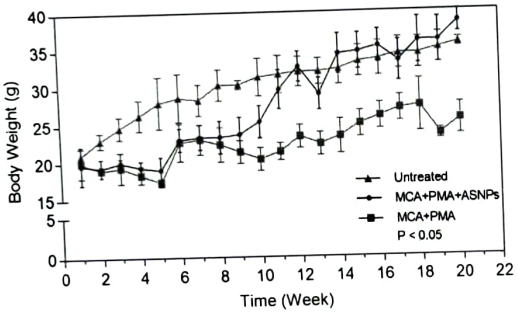

Figure 7: effect of AsNP in maintaining body weight growth in murine fibrosarcoma model

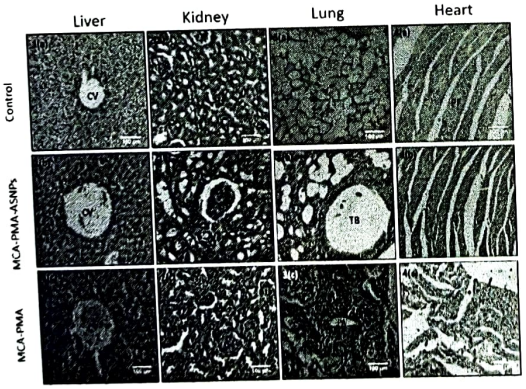

Figure 8: In the above Hematoxylin and Eosin stained micrograph shows the Central vein (CV) of liver, Glomerulus (G) of kidney, Terminal Branchiole (TB) of lung, pulmonary artery (PA) of lumg and purkinje fibres (PF) of heart.

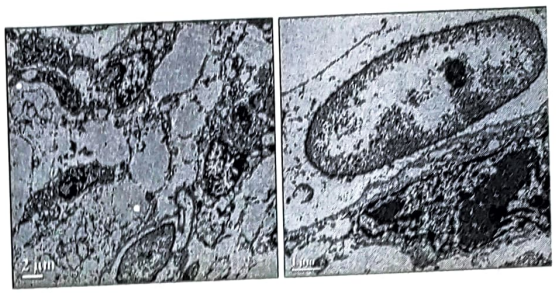

Figure 9: Transmission electron micrograph of tumor tissue after AsNPs Treatment showing canonical signs of apoptosis that includes pyknotic nuclei (Panel A). Microphotograph scale is 2 μm and 1 μm

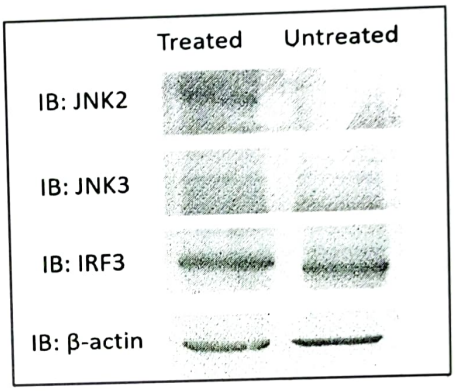

Figure 10: Figure showing western blot for JNK1, JNK2, β –actin and IRF3

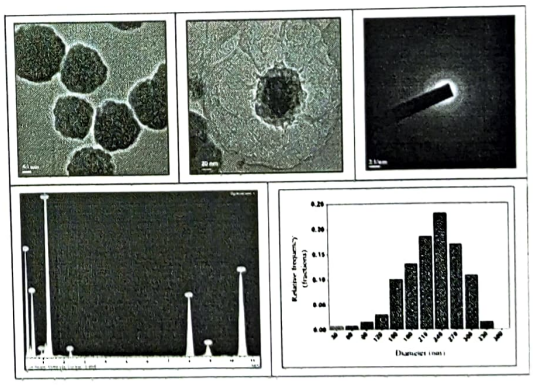

Figure 11: TEM micrograph and EDX of albumin coated ATONPs

Mahuya Sengupta 26/9/2018
Assistant Professor
Department of Biotechnology
Assam University
Silchar-788011

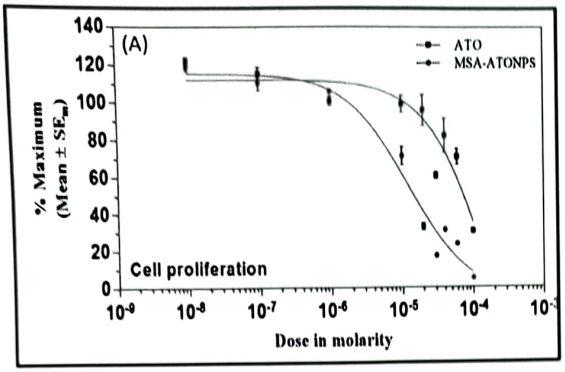

Figure 12: Non-linear regression curve plot showing the percentage of viable MCF7 cells determined by MTT assay after treatment with MSA-ATONPs and ATO with an increasing dose of MSA-ATONPs and ATO.

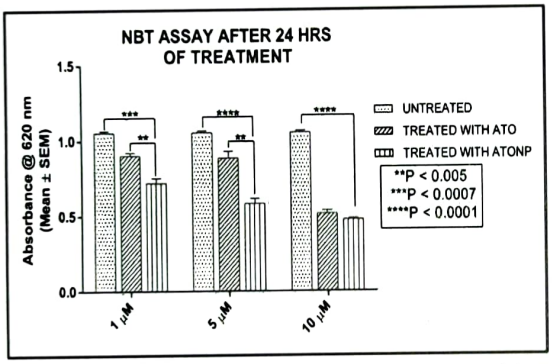

Figure 13: Decrease in mitochondrial metabolism of MCF7 cells 24 hours after treatment with ATONP & ATO.

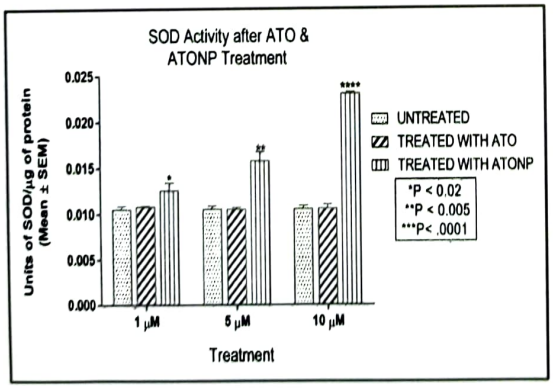

Figure 14: Increase in SOD activity 24 of MCF7 cells 24 hours after treatment with ATONP & ATO.

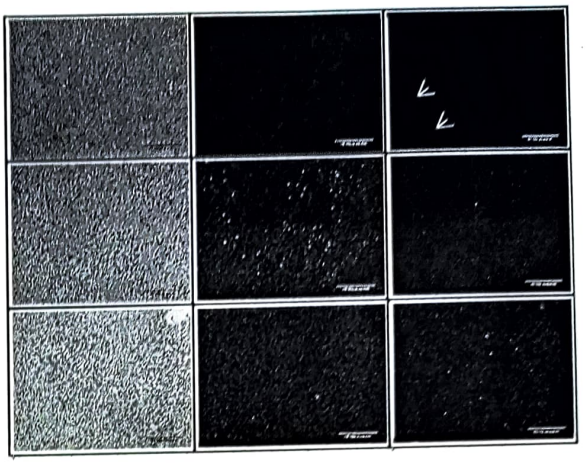

Figure 15: Annexin V-FITC {1(c), 2(c), 3(c)} and DAPI {1(b), 2(b), 3(b)} staining of untreated control {1(a)}, treated cells with 1 μM of ATONP {2(a)} and 5 μM of ATONP {3(a)}

Major organs	MSA-ATONP treated	ATO treated
Liver	242.041±5.736	<1 PPT
Plasma	211.057±9.475	<1 PPT
Tumor	200.084±14.112	<1 PPT
Spleen	114.017±12.030	<1 PPT
Kidney	91.638±3.407	<1 PPT
Lung	123.301±8.043	<1 PPT
Heart	66.594±6.108	<1 PPT

Table 1: Bio-distribution of arsenic quantified using ICP-MS

Mahuya Sengupta 26/9/2018
Assistant Professor
Department of Biotechnology,
Assam University
Silchar-788011

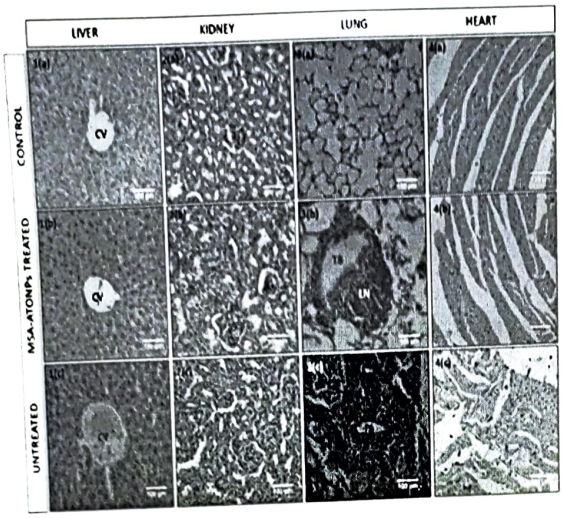

Figure 16: Hematoxylin and eosin (HE) stained micrograph of select organs carried out mainly for toxicity assessment after the MSA-ATONPs treatment. MSA-ATONPs treated mice retained normal tissue architecture as shown in Panel 1B for liver though some hyaline degeneration is visible whereas the untreated mice liver showed dilated central vein (CV) and hepatocytes with perinuclear clearing. Untreated mice kidney (Panel 3B) from tumor-bearing mice showed severe inflammation with dysplastic glomeruli and possible metastatic patches. Interestingly, the great reduction in severity is visible (Panel 2B) with the nanoparticle treatment. The lung from nanoparticle treated mice is shown in Panel 3B inflamed lymphatic nodule (LN) and restricted pulmonary micrometastasis but the lung from untreated mice (Panel 3C) displayed macro-metastasis and mucous filled alveoli. Micrograph in Panel 4B showing normal cardiac architecture with normal myocardium of nanoparticles treated mice. Microphotograph scale is 100 μm.

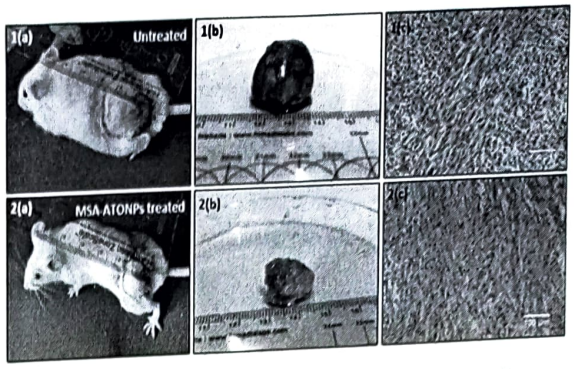

Figure 17: Reduced size of the tumor after ATONP treatment (2(a), (b)). H&E staining shows reduced density of nucleus in MSA-ATONP treated mice (2(c)) as compared to that of the ATONP untreated mice(1(c)). This suggests that less metastasis has occurred in MSA-ATONP treated mice.

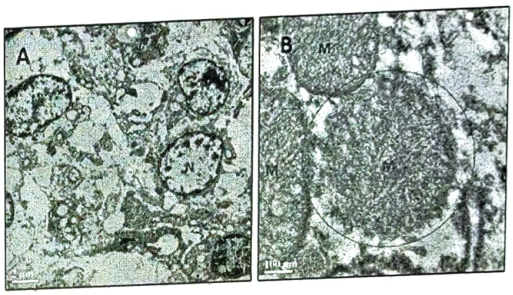

Figure 18: Transmission electron micrograph of tumor tissue after ATONP Treatment showing canonical signs of apoptosis that includes pyknotic nuclei (N) (Panel A) and ruptured mitochondrion (M) (Panel B). Microphotograph scale is 2 μm and 100 nm.

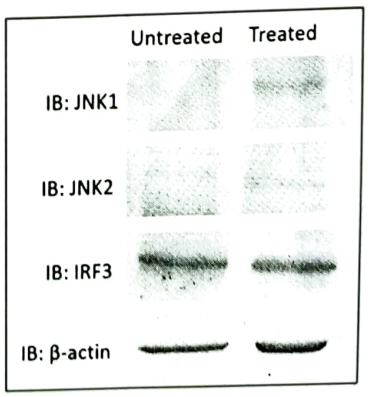

Figure 19: Immunoblots of JNK1, JNK2, IRF3 and b-actin

18

Mahuya Sengupta 26/9/2018
Assistant Professor
Department of Biotechnology
Assam University
Silchar-788011

Summary of the findings

This study was carried to analyse the immunomodulatory effects of arsenic nanoparticle (AsNp) on murine RAW 264.7 macrophage cell to validate the application of AsNP for targeting cancer. Pal et al. (2012) synthesized As(0) nanoparticle (AsNP) creating a new window in therapeutic prospect of Arsenic as chemotherapeutic agent. The particle was synthesized as per the published method and functionalized with albumin to increase the bio-availability and bio-efficacy by enhanced uptake. Initial cell viability assay shows as IC50 value AsNP is 1.3 X 10^{-4} M compared to 1.4 X 10^{-7} M of arsenic trioxide (ATO) making it a less toxic form of arsenical compound. This bioavailability finding was also correlated with other findings, which showed that coating nanoparticles with albumin reduces the chances of interaction with other serum proteins because albumin is the most abundant serum protein; thus, this functionalization enhanced the uptake by surrounding cells even at very low doses of nanoparticles [4, 5].Albumin has been used to increase the bioavailability of nanoparticles. Because of the structural homology among various types of albumin, bovine serum albumin was chosen to functionalize the AsNP.

This study showed that AsNP doses of 0.5 µM, 1 µM and 5 µM do not makes any significant change in nitric oxide production. But after stimulation with LPS; a well-known PAMP stimulates macrophage through TLR4, significantly increases nitric oxide production in untreated control. Whereas nitric oxide production and release was significantly lowered with AsNP treatment. Nitric oxide is known for its complex reactions with oxygen (O_2) or reactive oxygen species (e.g. superoxide O_2^-) yield numerous reactive nitrogens as well as oxygen species (RNOS), e.g., N_2O_3, peroxynitrite ($ONOO^-$), etc. These account for most of the so-called indirect effects attributed to nitric oxide through oxidation, nitrosation, and nitration reactions referred to as oxidative, nitrosative, and nitrative stress, respectively in tumor microenvironment[6]. Besides having two pronged character of nitric oxide in tumor *in situ* in both pro and anti-tumorigenic traits, iNOS mediated elevated level of nitric oxide in several tumor cases is correlated with its role in vasodilation and angiogenesis and play a dual role as both an effector molecule and upstream mediator of pro-tumorigenic cytokine release such as TNF-α and other proinflammatory events[7]. Our study shows that AsNP do not interfere with the constitutive nitric oxide production important for cell signaling and immune reactions but dramatically reduce nitric oxide production after LPS stimulation by limiting iNOS activity which might be through NF-κβ mediated.

One of the prime facts of tumor promotion and surveillance is that immune cells (especially macrophages) associated with the tumor microenvironment mainly promote the tumor[8]. Thus, the AsNP treatment to the immune cells or other cells induces oxidative stress, which may collectively contribute to the anticancer response. The explanation is supported by the *in vitro* findings of increased expression of SOD at protein level after treatment, what may be considered as AsNP induced oxidative stress.

A comparative study of arsenic trioxide and arsenic trioxide nanoparticle confirmed induction of apoptosis on MCF 7 cell most probably through oxidative pathway as confirmed from oxidative stress marker: SOD activity and is significantly comparable with arsenic trioxide. JNK (Jun-N-terminal kinase):

Mahuya Sengupta 26/9/2018
Assistant Professor
Department of Biotechnology
Assam University
Silchar-788011

Hematoxylin and eosin (HE) stained micrograph of select organs carried out mainly for toxicity assessment after the AsNPs treatment. Hematoxylin has a deep blue-purple color and stains nucleic acids by a complex, incompletely understood reaction. Eosin is pink and stains proteins nonspecifically. In a typical tissue, nuclei are stained blue, whereas the cytoplasm and extracellular matrix have varying degrees of pink staining (Fischer et al., 2008). Histological study using HE staining shows AsNPs treated mice retained normal tissue architecture for liver, though some hyaline degeneration is visible whereas the untreated mice liver showed dilated central vein (CV) and hepatocytes with perinuclear clearing. Untreated mice kidney from tumor-bearing mice showed severe inflammation with dysplastic glomeruli and possible metastatic patches. Interestingly, the great reduction in severity is visible with the nanoparticle treatment. The lung from nanoparticle treated mice is shown inflamed lymphatic nodule (LN) and restricted pulmonary micrometastasis but the lung from untreated mice displayed macro-metastasis and mucous filled alveoli. Micrograph of heart shows normal cardiac architecture with normal myocardium of nanoparticles treated mice.

By western blot analysis the expression of cellular protein is analyzed and the presence of β –actin, IRF3 and JNK is detected. 1st one is the loading control. The absence of band in the membrane requires proof that protein is present in each lane of the gel but our protein of interest is missing. A control antibody, or loading control (LC) often serves this purpose. Antibodies against β-actin and glyceraldehyde 3-phosphate dehydrogenase (GAPDH), along with other high-abundance housekeeping proteins, are used. Equal intensity of bands for the expression of β –actin in the samples shows that there is no loading error or any experimental error in our study.

a. JNK (Jun-N-terminal kinase): The bands for JNK expression have been detected in AsNPs sample while the AsNPs untreated sample has not shown any band for JNK, suggesting alterations in the cytokine signaling cascades. As JNK also induces apoptosis in cells under stressed conditions, the result suggests that AsNPs has a role in induction of apoptosis via JNK pathway, corroborated by canonical signs of apoptosis in the treated cells, like membrane blebbing, ruptured mitochondria, presence of apoptotic bodies and pyknotic nuclei.

b. IRF3: IRF3 is activated via TLR signalling pathway in response to any stress and leads to the production of cytokines. The equal expression for IRF3 expression in both treated and untreated sample inferred that AsNP has not induced any significant change in the TLR signalling pathway in tumour cells

To exploit the anti-cancer properties of ATO, the study is focused on initiation of cell death by ATO but at relatively lower concentration and improved bioavailability. In order to employ inherent pro-apoptotic property associated with ATO induced intracellular signalling, we synthesized and characterized a bioactive nanoparticulate form of ATO to challenge the difficulties associated with its toxic nature. Our study establishes the improved pro-apoptotic and anti-proliferative property of ATO in the form of MSA-ATONPs with minimal side effects.

ICP-MS data showed distribution and accumulation of MSA-ATONPs in tumor. Accumulation in the tumor may be contributed to the leaky vascularity,(Dvorak et al., 1988; Jain, 2005) and overexpressed albumin receptors in the cancer cells, ready targets of the albumin-coated nanoparticles.

Mahuya Sengupta 26/9/2018
Assistant Professor
Department of Biotechnology
Assam University
Silchar-788011

Although liver tissue showed maximum accumulation, histopathology of liver did not show any inflammation or necrotic patches but retained normal tissue architecture. The possible protective mechanism is the xenobiotic biotransformation of As(III) to less cytotoxic methylated As(V) in the hepatic cells that is excreted with bile (Hayakawa et al., 2005; Lin et al., 2002) Accumulation of the particles in plasma reveals retention mostly because of reduced renal clearance. The increased accumulation in tumor and reduced plasma clearances is also attributed to the particulate nature and surface functionalization of ATONPs with albumin.(Kratz, 2008; Li and Huang, 2008) Relatively high amount of arsenic in lung is possibly due to pulmonary micrometastases (Gao et al., 2008; Renoux and RENOUX, 1972) potential targets of the albumin-coated nanoparticles (Merlot et al., 2014) Albumin being the most abundant plasma protein, shields the interaction of the NPs with the blood cells and other plasma constituents

The transmission electron micrograph of the tumor of ATONP treated mice showed significant number of dead cells. This clearly suggests that treatment with ATONP has lead to the apoptosis of the tumor cells.

As2O3 induced apoptosis via the loss of the mitochondrial membrane potential. Nanoparticles are taken up by the cells via endocytosis forming an endosome inside the cell. Lysosomes then fuse with the endosome containing nanoparticle and forms endolysosome. Endolysome then attacks mitochondria resulting into the mitochondrial membrane breakdown releasing cytochrome c into the cytosol where it binds and activates Apaf-1, which in turn activates procaspase-9. Caspase-9 cleaves procaspase-3, and downstream of caspase-3, the apoptotic program branches into a multitude of subprograms, the sum of which results in the ordered dismantling and removal of the cell.

Hematoxylin and eosin (HE) stained micrograph of select organs carried out mainly for toxicity assessment after the MSA-ATONPs treatment. Hematoxylin has a deep blue-purple color and stains nucleic acids by a complex, incompletely understood reaction. Eosin is pink and stains proteins nonspecifically. In a typical tissue, nuclei are stained blue, whereas the cytoplasm and extracellular matrix have varying degrees of pink staining. Histological study using HE staining shows MSA-ATONPs treated mice retained normal tissue architecture for liver, though some hyaline degeneration is visible whereas the untreated mice liver showed dilated central vein (CV) and hepatocytes with perinuclear clearing. Untreated mice kidney from tumor-bearing mice showed severe inflammation with dysplastic glomeruli and possible metastatic patches. Interestingly, the great reduction in severity is visible with the nanoparticle treatment. The lung from nanoparticle treated mice is shown inflamed lymphatic nodule (LN) and restricted pulmonary micrometastasis but the lung from untreated mice displayed macro-metastasis and mucous filled alveoli. Micrograph of heart shows normal cardiac architecture with normal myocardium of nanoparticles treated mice.

Western blotting has been performed to detect the expression of few target proteins in cancer cells. β –actin has been used as the loading control because the absence of band in the membrane requires proof that protein is present in each lane of the gel but our protein of interest is missing. A control antibody or loading control (LC) often serves this purpose.

JNK (Jun-N-terminal kinase): The bands for JNK expression have been detected in

Mahuya Sengupta 26/9/2018
Assistant Professor
Department of Biotechnology
Assam University
Silchar-788011